Improvement of the isothermal oxidation resistance of CoNiCrAlY coating sprayed by High Velocity Oxygen Fuel

Surface & Coatings Technology 204 (2010) 3723–3728

Contents lists available at ScienceDirect

Surface & Coatings Technology

journal homepage: www.elsevier.com/locate/surfcoat

Improvement of the isothermal oxidation resistance of CoNiCrAlY coating sprayed by High Velocity Oxygen Fuel

Alessio Fossati [a,*], Martina Di Ferdinando [a], Alessandro Lavacchi [b], Ugo Bardi [a], Carlo Giolli [c], Andrea Scrivani [c]

[a] INSTM – Consorzio Interuniversitario Nazionale per la Scienza e Tecnologia dei Materiali, Via G. Giusti 9, 50121 Firenze, Italy
[b] Istituto di Chimica dei Composti Organometallici (ICCOM-CNR), Via Madonna del Piano 10, 50019 Sesto Fiorentino, Italy
[c] Turbocoating SpA, V. Mistrali 7, 43040 Rubbiano di Solignano, Parma, Italy

ARTICLE INFO

Article history:
Received 23 March 2010
Accepted in revised form 23 April 2010
Available online 20 May 2010

Keywords:
High Velocity Oxygen Fuel (HVOF)
Oxidation
Superalloy
Bond coat
Protective coating

ABSTRACT

Two CoNiCrAlY powders with similar chemical composition and granulometry, but with different starting reactivity toward oxygen, were sprayed by High Velocity Oxygen Fuel (HVOF) onto Hastelloy X superalloy substrates obtaining coatings of comparable thickness. After spraying, samples were maintained at 1000 °C in air for different test periods up to 3000 h. Morphological, microstructural, compositional and electrochemical analyses were performed onto the powders and the coated samples in order to assess the high temperature oxidation resistance provided by the different powders. The powder with higher starting reactivity toward oxygen sensibly improves the oxidation resistance of the coated samples by producing thinner and more adherent thermally grown oxide layers in comparison with the other powders.

1. Introduction

Thermal barrier coating (TBC) systems are widely used in gas turbines in order to reduce thermal exposure of structural components and increase turbine efficiency. TBCs are usually composed of a MCrAlY bond coat (with M = Co, Ni or their combination) as an oxidation resistant layer and an yttria partially stabilized zirconia (YPSZ) top coat that provides thermal insulation to the metallic substrate. In addition, the bond coat enhances the adhesion of the ceramic top coat. The performance of the bond coat is limited in time: after a certain period in working conditions, oxidation of the bond coat causes the development of a thermally grown oxide (TGO) layer at the ceramic/bond coat interface. The formation of this TGO layer has been recognized to be one of the main causes for the TBC failure [1–3]. Failure of the TBC coating critically depends on the characteristics of the TGO layer. If this layer is composed of a continuous, compact and adhesive alumina (Al_2O_3) scale, it acts as a diffusion barrier; moreover, the alumina scale can suppress or reduce the growth of other detrimental oxides and protect the substrate from further oxidation, improving the system service life [4–7]. Many researches showed that TBC failures can be correlated to the reaching of a TGO critical thickness [8,9]. Thus, producing bond coats with low TGO thickening rate can have a significant impact on the durability of TBC system [10].

The characteristics of the bond coat in terms of resistance to oxidation and morphology of the TGO depend not only on the chemical composition but also on the method used to create the coating. MCrAlY coatings can be produced by several thermal spraying techniques (VPS, APS, LPPS and HVOF). VPS (Vacuum Plasma Spraying) represents the state of the art technology for the industrial bond coat deposition, but the cost is relatively high due to the vacuum operation condition. VPS avoids the aluminium oxidation during the spraying and the relative consumption of the Al reservoir of the coating before the service life.

HVOF spray systems work at atmospheric pressure and consequently the investment and operation costs are much lower [11–15]. Recent researches showed the potentiality of HVOF spraying system compared to VPS technique [16]. Other studies attribute to the HVOF process the capability of forming a fine Al_2O_3 dispersion during the spraying process [17]. The presence of alumina nuclei in the as-deposited coating seems to have a beneficial effect on the oxidation resistance by promoting the growth of a protective TGO layer. In this sense, the HVOF spraying of powders with high oxygen affinity could result suitable in the industrial production of bond coats not just because of the lower costs but also in terms to produce higher oxidation resistant TBCs.

In the present work, two different bond coats of comparable thickness, were deposited onto a superalloy substrate by means of HVOF systems, using two different CoNiCrAlY powders with about the same chemical composition and granulometry, but showing different

* Corresponding author. Dipartimento di Chimica, Università degli Studi di Firenze, via della Lastruccia 3, 50019 Sesto Fiorentino (FI), Italy. Tel.: +39 0554573119; fax: +39 0554573120.
E-mail address: alessio.fossati@gmail.com (A. Fossati).

0257-8972/$ – see front matter © 2010 Elsevier B.V. All rights reserved.
doi:10.1016/j.surfcoat.2010.04.059

starting reactivity toward oxygen. After deposition, the samples were isothermally oxidized at 1000 °C for different periods of time up to 3000 h. Before and after the furnace tests, the samples were extensively characterized. The different properties and characteristics of the powders and the coatings were analyzed and discussed.

The aim of the present work is to investigate how the initial powder reactivity toward oxygen can affect the final oxidation behavior of bond coats produced by HVOF technique.

2. Material and methods

Hastelloy X nickel based superalloy (with a nominal composition of: Ni balance, Cr-22, Fe-18, Mo-9, Co-1.5, W-0.6, Si<1 (wt.%)) squared samples (25×25 mm), were used as substrates. Before deposition, the substrates were grit blasted using corundum with a grain size of 60–80 mesh, in order to remove surface oxides and to obtain a suitable roughness for coating adhesion.

The composition of the two CoNiCrAlY powders (hereafter named "A" and "B") are reported in Table 1.

The as-received powders were characterized by scanning electron microscopy (SEM), energy dispersive X-ray microanalysis (EDX), X-ray diffraction (XRD) and thermal gravimetric analysis (TGA). TGA was performed at 1000 °C in air (flux: 20 ml/min, heating rate to the temperature set point: 15 °C/min for about 20 h recording the mass gain due to the oxide layer formation. Weight gains for each kind of powder were normalized considering the total surface area exposed to the aggressive environment. The total area was estimated by the data obtained by means of laser granulometric analysis.

The torch used to manufacture the bond coats was a liquid fuelled gun (Tafa/Praxair JP5000); the powder injection was radial and the gas flow was obtained by the combustion between oxygen and kerosene.

After spraying, all the samples were subjected to a vacuum interdiffusion treatment for 2 h at 1150°C.

Isothermal oxidation tests of the two different coated specimen types were conducted at the same time and in the same high temperature furnace at 1000°C in air, in order to assure identical test conditions. Samples were analyzed before and after 500, 1000, 2000 and 3000 h of test. The cooling down of the samples was carried out inside the furnace reaching about the room temperature by 24 h.

The average thickness of the coatings, the interdiffusion layer and Al depletion layers were measured by optical and scanning electron microscopy (SEM). The surface morphology and the chemical composition of the as-coated and oxidized samples were examined by SEM-EDX. XRD analysis (Bragg–Brentano configuration using Cu-Kα radiation) were performed on the surface of the coatings, in order to determine the crystalline structure and estimate the relative amount of the main surface phases, before and after the different oxidation exposition times.

EIS (electrochemical impedance spectroscopy) analysis was performed before and after 500, 1000, 2000 and 3000 h of test. The measurements were carried out on 3 different samples for each sample type in order to assess the reproducibility. EIS measurements were carried out at room temperature in a conventional three-electrode system in a flat cell with a volume of 300 ml. Coated samples were used as working electrodes exposing to the electrolyte an area of 1 cm^2. A platinum mesh was used as a counter electrode and a KCl-saturated Calomel electrode was used as reference. $K_3Fe(CN)_6/K_4Fe(CN)_6$ aqueous solution (0.01 M) was employed as electrolyte, because of its highly reversible electrochemical exchange current density and minimal interference with the system [18]. A sinusoidal voltage perturbation of 15 mV amplitude and a frequency range of 50 mHz–100 kHz was selected. EIS measurements were performed at the open circuit potential after a delay period from 1 to 24 h in order to assess the stability of the system.

Table 1
Chemical composition of the powders A and B.

Powder type	%Co	%Ni	%Cr	%Al	%Y	%Ca	%Si
A	Balance	31.3	20.9	8.0	0.54	–	–
B	Balance	32.0	21.1	8.3	0.53	0.085	0.028

3. Results and discussion

3.1. Powder characterization

The powder particle size ranged between 15 and 45 μm for both the powder types.

Both the powders showed a spherical morphology and mainly consisted of two metallic phases (γ-(Co,Ni) and β-(Co,Ni)Al) as shown in Fig. 1. Nevertheless it has to be noted that the crystallite size of powder B was smaller in comparison with powder A, as revealed by the broadening of the diffraction peaks.

The powders' composition was very similar, except for the presence of small amounts of silicon and calcium in powder B.

The TGA analysis results are reported in Fig. 2. The graph shows a higher mass gain in the case of powder B. Particularly, the mass gain is concentrated during the first stages. This behavior suggests that, during the spraying, powder B could tend to oxidize much more in respect to powder A. Generally, this feature it is not considered beneficial for the durability of coatings, because it is thought that the aluminium oxidation during the spraying results in an Al reservoir depletion. The hypothesis here, instead, is that a higher reactivity toward oxygen could improve the quality of the TGO and promote a subsequent higher oxidation resistance.

3.2. Bond coat characterization

In the following, we present results comparatively for each type of studied feature. Bond coats obtained by spraying powders A and B will be hereafter respectively named samples A and samples B.

3.2.1. Al depletion zones and TGO growth

Fig. 3 shows some micrographs of the sample cross sections before and after different oxidation periods of time. The overall thickness of the sample bond coats was about 300 μm. The as-coated samples

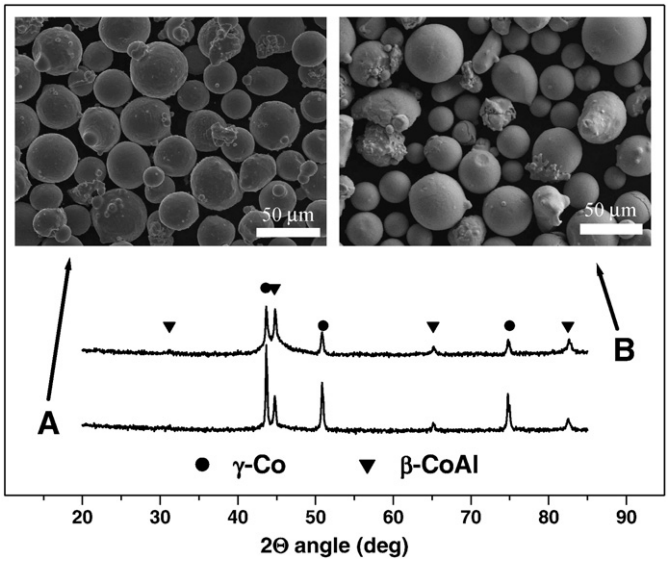

Fig. 1. XRD patterns and SEM micrographs of powders A and B.

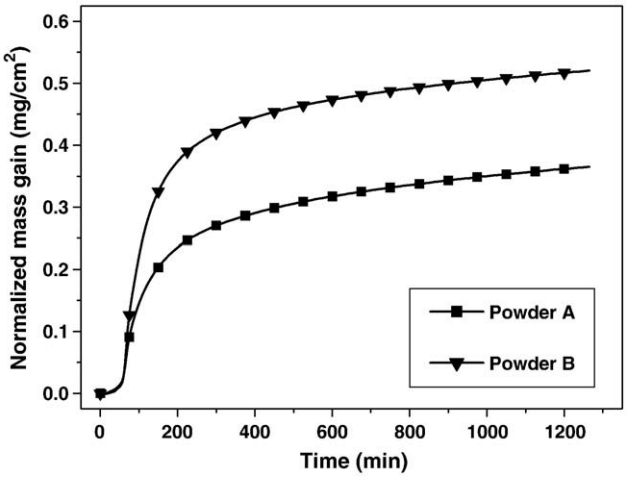

Fig. 2. Comparison between TGA curves of powders A and B.

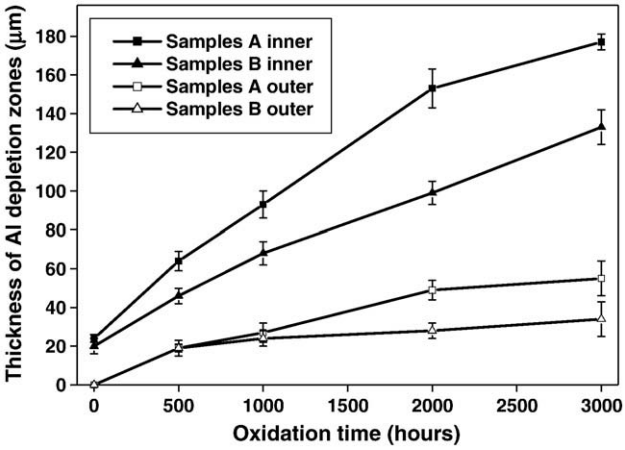

Fig. 4. Thickness of the inner and outer aluminium depletion layers of samples A and B before and after different periods of oxidation at 1000 °C.

showed both the γ and β phases present in the powders. A thin interdiffusion layer (about 20 μm) was detected between the bond coat and the superalloy. During oxidation, Al diffused out of the CoNiCrAlY coating surface to form the TGO layer and into the substrate, promoting outer and inner β-(Co,Ni)Al depletion. The Al depletion zone thickness increased during the tests.

In Fig. 4 the thickness of the outer and inner Al depletion zones before and during the oxidation tests are reported. EDX analysis performed in the Al rich zones of both the samples showed an Al concentration comparable to the initial values. In the case of samples of type A, after 3000 h at 1000 °C, the Al reservoir is quite completely depleted and the residual life, before the start of severe oxidation phenomena with the Cr_2O_3 formation, could be reasonably estimated in about additional 500 h. On the contrary, in the case of samples of type B, the Al reservoir is still efficient and the residual life could be estimated over additional 1500 h.

Both sample types showed larger inner depletion layers in comparison with the inner ones. This behaviour can be ascribed to the high Al concentration gradient between the bond coats and substrate (Hastelloy X does not contain sensible amount of aluminium). By using a superalloy substrate containing some aluminium percentages the service life of the coatings can be enhanced sensibly by limiting aluminium diffusion into the bulk.

Moreover, it has to be noted that both inner and outer aluminium depleted zones of samples B, showed a slower increasing rate in comparison with samples A. The slower growth rate of the outer zone could be correlated to a higher oxidation resistance of the samples B, due to a more protective TGO, which allows a smaller aluminium consumption from the bond coat reservoir.

The reduced diffusion into the bulk cannot be explained in terms of oxidation resistance, because diffusion depends only on the concentration gradient and on the aluminium diffusion coefficients. The fact that aluminium diffuses into the bulk at a lower rate in the case of samples B could be ascribed to lower apparent diffusion coefficients — this conclusion derives from the fact that the gradient concentration can be reasonably considered approximately the same in both types of samples. This behaviour could be related to the formation of a diffusion barrier layer between the splats during the spraying. Probably, powder B, which can be easily oxidized during the spraying, is able to produce, at the fly time, a thin aluminium oxide layer which works as a diffusion barrier, limits the aluminium diffusion coefficients and allows a slower aluminium diffusion through the coating toward the substrate.

In Fig. 5 the thickness evolution of TGO layers of the two different coating types are reported as measured in zones where no evident fracture and delamination signs were detected. The TGO thickness of

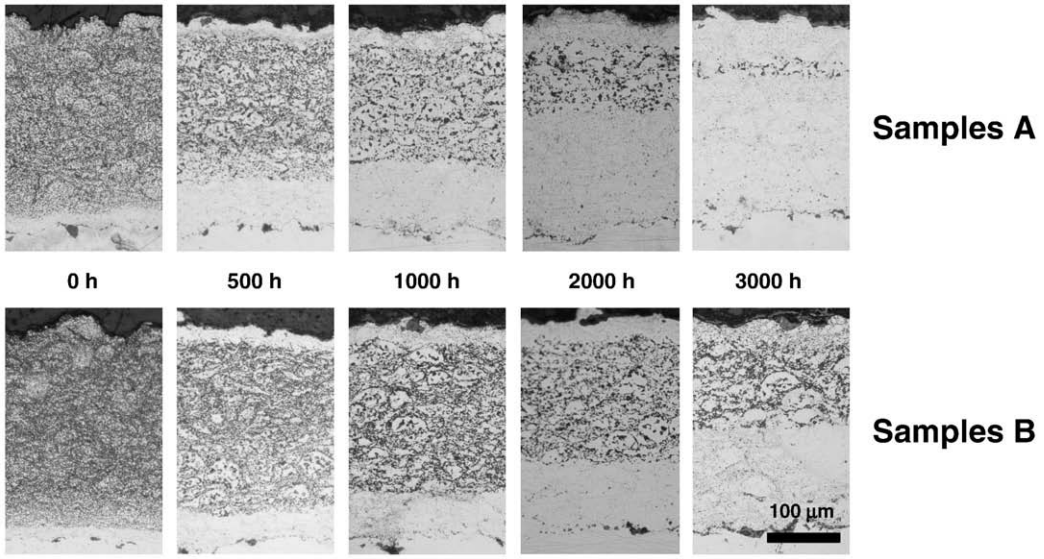

Fig. 3. Optical micrographs of the cross sections of the samples produced with powders A and B after different periods of oxidation at 1000 °C.

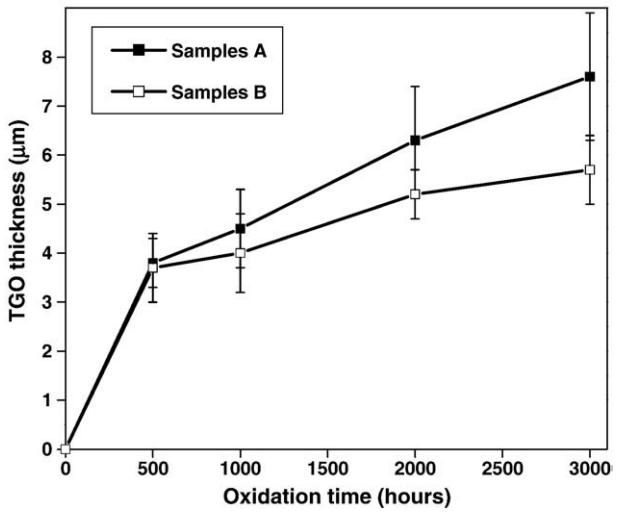

Fig. 5. Thickness of TGO layers of samples A and B after different periods of oxidation at 1000 °C.

samples B was always smaller in comparison with samples A. It is likely that the samples B result in more compact and adhesive TGO layers.

3.2.2. Surface modifications

In Fig. 6 it is shown a picture which allows a visual comparison of the surfaces of the samples before and after the oxidation test. Before the test, the bond coats had a metallic appearance. Oxidation phenomena generate a blue coloration, due to the presence of cobalt which reacts with oxygen.

Visual inspection of samples A revealed the first signs of TGO delamination after just 1000 h of test. Delamination phenomena sensibly increased after 2000 h, when a large percentage of surface oxide spalled out and the surface lost the prevalent blue coloration. On the contrary, samples B, showed only minor delamination signs after 2000 h of test and did not show relevant oxide spalling even after 3000 h.

It is reasonable to think that most of the delamination phenomena occurred during the cooling down to the room temperature, despite the very low cooling rate. Thus, visual inspection allows to coarsely evaluate the higher adhesion of the TGO layers formed onto samples B in comparison with samples A. The better adhesion could be ascribed both to the lower thickness and to the higher quality of the TGO of samples B in respect of the other type.

In Fig. 7 SEM micrographs of the coated samples before and after different periods of oxidation are shown. The coatings showed a rough surface, due to the overlap of different splats and to the roughness of each single splat. Increasing the oxidation time, nucleation and growth of the oxide scale became more and more significant, as showed by the sample charging under the electron beam. Moreover, some delaminations of the TGO layers can be observed. According to the visual inspection samples A show larger detached areas in comparison with samples B.

XRD analysis performed onto the as-coated samples showed the occurrence of both the γ and β phases (Fig. 8). Even after 3000 h of oxidation tests, the XRD patterns indicated that the oxide scale was mainly constituted of α-Al_2O_3 and $(Co,Ni)(Cr,Al)_2O_4$ spinel for each sample type. No Cr_2O_3 peaks were detected, according to the cross sectional analysis which did not show the starting of severe oxidation phenomena.

In Fig. 9 the results of EDX analysis performed onto the surface of untested and oxidized samples are reported. Untested samples showed an Al concentration higher in comparison with that of the original CoNiCrAlY powders. This behaviour can be ascribed to the preferential aluminium oxidation during the spraying or the low vacuum interdiffusion treatments. Nevertheless the oxide layers are certainly very thin in agreement with the visual inspection and the XRD analysis that did not detect a sensible amount of oxides. During the first 500 h of the oxidation tests the surface aluminium concentration sensibly increases due to scale formation. After this initial period, some relevant differences occurred to the different samples. The compositional analysis shows that the aluminium and nickel content, respectively, decreases and increases more rapidly in samples A in comparison with samples B. This behaviour can be correlated with the delamination of the oxide layers which expose to the microprobe more internal layer. After 1000 h of test, the chromium concentration of samples A seems to increase more rapidly in comparison with that of samples B. This can be ascribed to the growing of chromium containing oxides, such as the spinel revealed by XRD analysis. After 1000 h, the surface chromium concentration of samples A did not increase; probably as the result of delamination phenomena. Generally, the surface composition of samples B measured by EDS appeared more stable in agreement with the lower growth rate of the TGO layer and to the absence of relevant spalling phenomena.

3.2.3. EIS measurements

Electrochemical impedance spectroscopy results will be not presented trying to fit data with some electrical equivalent circuit.

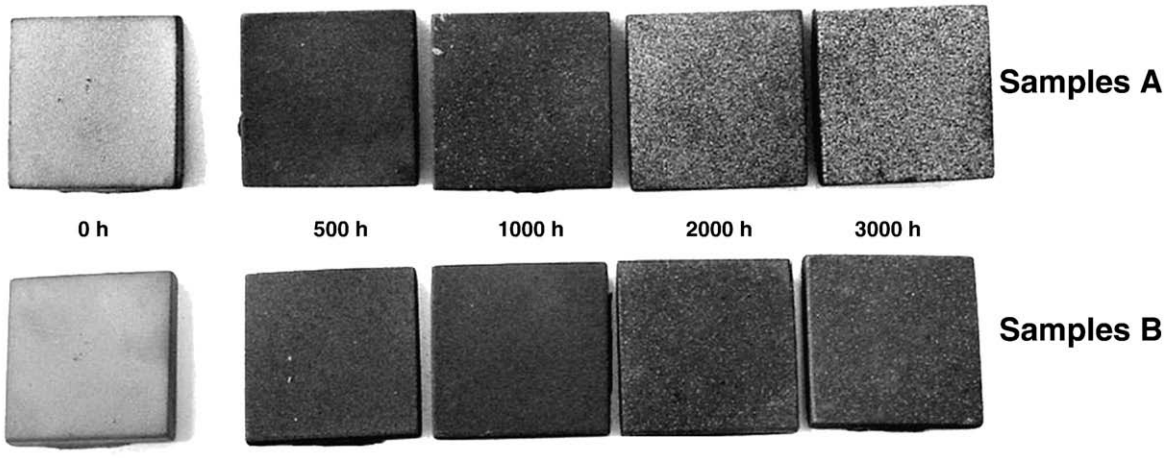

Fig. 6. Picture showing the typical appearance of samples A and B before and after different periods of oxidation at 1000 °C.

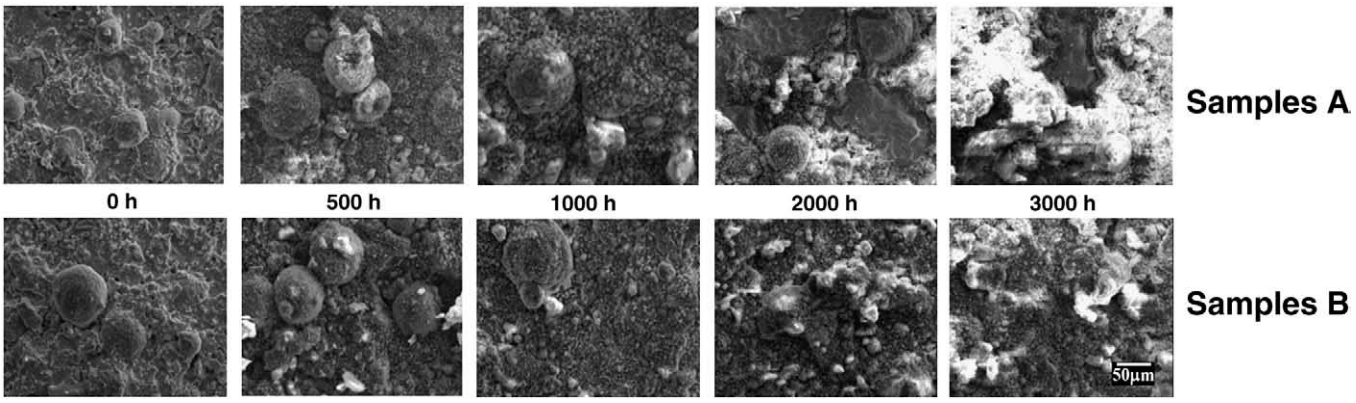

Fig. 7. SEM micrographs showing the morphology evolution of the surface of samples A and B before and after different periods of oxidation at 1000 °C.

In this work the interest is the simple comparison of the different curves, measured after different oxidation periods onto the 2 different coating types, in order to obtain some general considerations about the growth and quality of the TGO layer.

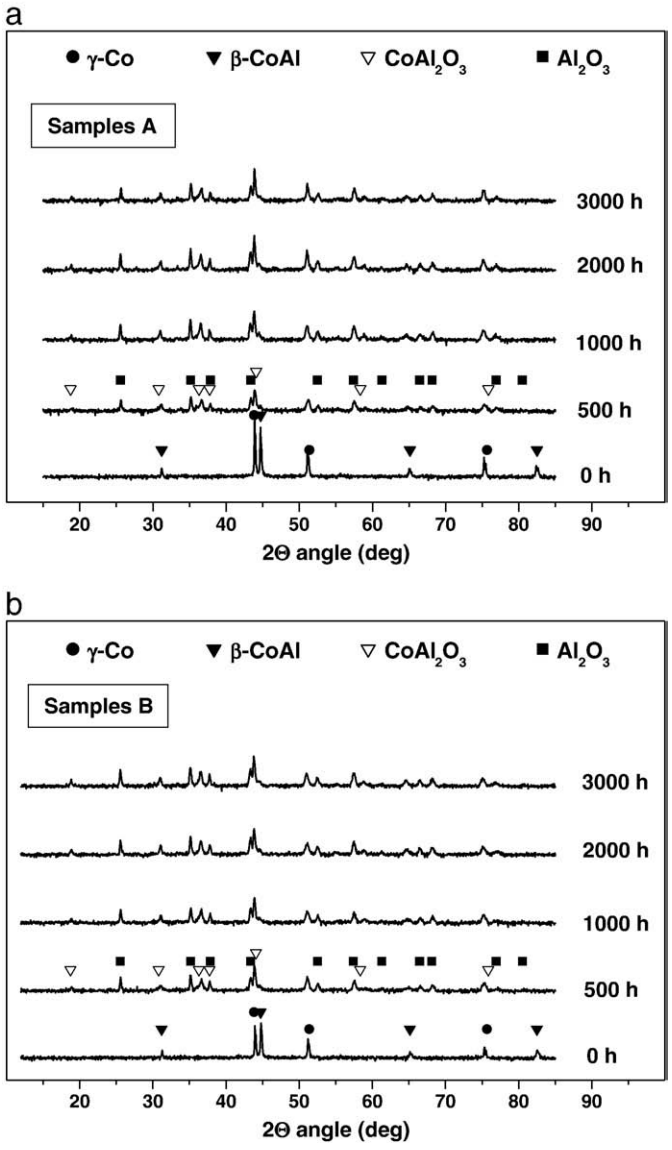

Fig. 8. XRD patterns of the surface of samples A (a) and B (b) before and after different periods of oxidation at 1000 °C.

The Fig. 10 shows that the electrochemical impedance values of samples A increased from the untreated samples to the samples oxidized for 500 h, then an impedance value decrease occurred. Particularly, samples oxidized for 3000 h showed impedance values comparable with those of the untreated ones.

In the case of samples B a different behaviour was observable. The electrochemical impedance increased passing from the untested samples to the samples oxidized for 500 h and reaches the maximum values in the case of samples tested for 1000 h. Then the impedance

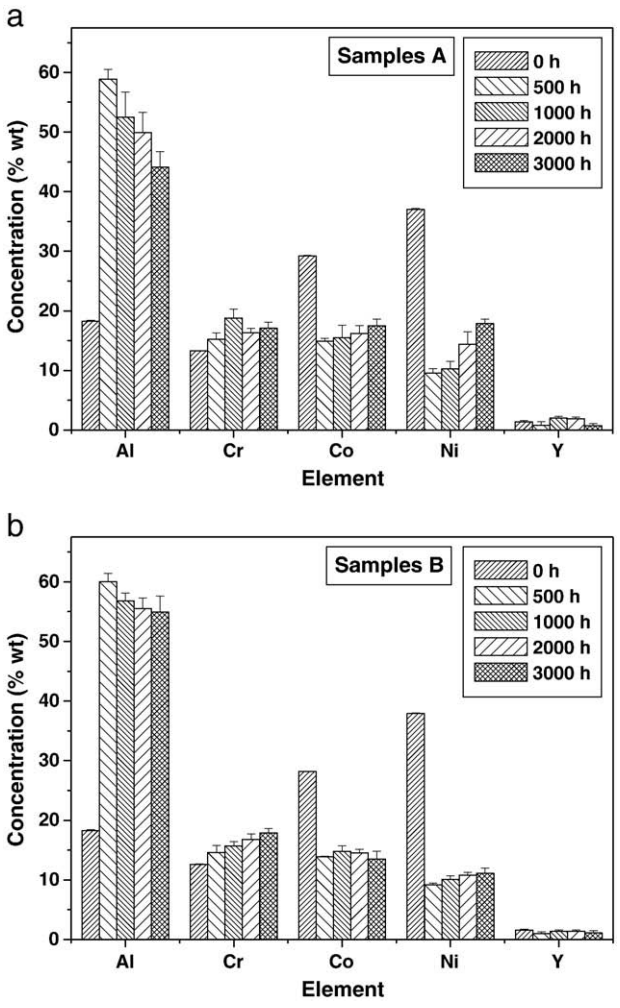

Fig. 9. Surface composition measured by EDS analysis of samples A (a) and B (b) before and after different periods of oxidation at 1000 °C.

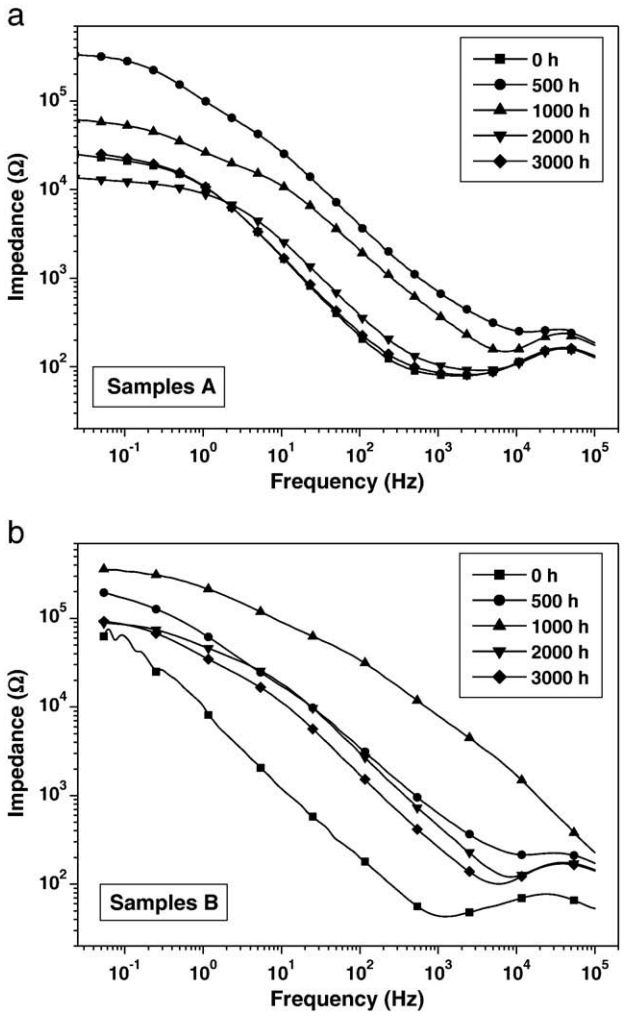

Fig. 10. EIS Bode plot of samples A (a) and B (b) before and after different periods of oxidation at 1000 °C.

values decreased, but even in the case of samples oxidized for 3000 h the impedance values are higher than those of the untreated samples.

The different behaviour of samples A and B can be mainly ascribed to the differences of adhesion of the two different coatings. The impedance values can be primarily correlated with thickness and quality of the coatings. A compact and scarcely defective TGO layer increases the electrochemical impedance values of the samples as its thickness increases, due to the lowering of the electrical capacity and to the increasing of its electrical resistance. It is reasonable to suppose that the impedance values of samples with a delaminated TGO layer are intermediate between those of samples with a defect free TGO layer and the bare substrate without any oxide layer.

Samples B showed a higher quality of the TGO layer; their thickness increase produced higher impedance, thanks to the minor level of delamination.

In the case of samples A even if there is a TGO thickness increment, this is accompanied by delamination phenomena just after the first periods of the test. This did not allow the increase of the impedance values, because of the averaging effect between the non-defective TGO impedance and that of the damaged zones. According to visual and microscopic inspections, samples A after 3000 h of test showed a surface with a very large percentage of delamination areas, while samples B did not. The large TGO delamination can explain impedance values very similar to those of the unoxidized samples.

At last, it has to be noted that electrochemical impedance analysis is a very sensible tool in order to study and assess the quality of the TGO layer. Particularly its sensitivity is higher in comparison with visual inspection, microscopic techniques and XRD analysis and allowed to estimate the starting of delamination phenomena before of the other techniques. These results corroborate the idea that EIS analysis can be used as a non destructive evaluation instrument in order to study the residual life of complete TBC systems.

4. Conclusions

In this work isothermal high temperature oxidation tests of CoNiCrAlY bond coats of comparable thickness produced by HVOF onto Hastelloy X substrates were carried out. The two powders used to produce the different coatings had about the same chemical composition and granulometry, but different starting reactivity toward oxygen.

Morphological, microstructural, compositional and electrochemical analyses were performed in order to characterize the samples before and after the oxidation tests. The results showed considerable differences in the behaviour of the two powders. Bond coats produced by means of the powders with higher starting reactivity toward oxygen resulted in sensibly higher oxidation resistance and adhesion in comparison with the other one. This behaviour could be ascribed to the formation of alumina precursor nuclei on the splat surface which promotes adherent and good quality oxide scale growth and act as a diffusion barrier of aluminium toward the substrate.

Acknowledgements

This work was supported by the FIRB Project no. RBIP06X7F4.

References

[1] W. Brandl, H.J. Grabke, D. Toma, J. Krüger, Surf. Coat. Technol. 86–87 (1996) 41.
[2] A.G. Evans, D.R. Mumm, J.W. Hutchinson, G.H. Meier, F.S. Pettit, Prog. Mater. Sci. 46 (2001) 505.
[3] E.A.G. Shillington, D.R. Clarke, Acta Mater. 47 (1999) 1297.
[4] M.J. Stiger, N.M. Yanar, M.G. Toppings, F.S. Pettit, G.H. Meier, Z. Metall. 90 (1999) 1069.
[5] N. Padture, M. Gell, E. Jordan, Science 296 (2002) 280.
[6] R.A. Miller, J. Therm, Spray Technol. 6 (1997) 35.
[7] D.R. Clarke, C.G. Levi, Annu. Rev. Mater. Sci. 33 (2003) 383.
[8] A.G. Evans, D.R. Mumm, J.W. Hutchinson, G.H. Meier, F.S. Pettit, Prog. Mater. Sci. 46 (2001) 505.
[9] E.P. Busso, J. Lin, S. Sakurai, M. Nakayama, Acta mater. 49 (2001) 1515.
[10] W.R. Chen, X. Wu, B.R. Marple, D.R. Nagy, P.C. Patnaik, Surf. Coat. Technol. 202 (2008) 2677.
[11] W.R. Chen, X. Wua, B.R. Marple, D.R. Nagy, P.C. Patnaik, Surf. Coat. Technol. 202 (2008) 2677.
[12] R. Taylor, J.R. Brandon, R. Taylor, P. Morrell, Surf. Coat. Technol. 50 (1992) 141.
[13] D. Toma, W. Brandl, U. Köster, Surf. Coat. Technol. 120–121 (1999) 8.
[14] W. Brandl, D. Toma, J. Kruger, H.J. Grabke, G. Matthaus, Surf. Coat. Technol. 94–95 (1997) 21.
[15] E. Lugscheider, C. Herbst, L. Zhao, Surf. Coat. Technol 108–109 (1998) 16.
[16] M. Di Ferdinando, A. Fossati, A. Lavacchi, U. Bardi, F. Borgioli, C. Borri, C. Giolli, A. Scrivani, Surf. Coat. Technol. 204 (2010) 2499.
[17] F.H. Yuan, Z.X. Chen, Z.W. Huang, Z.G. Wang, S.J. Zhu, Corros. Sci. 50 (2008) 1608.
[18] J. Gómez-García, A. Rico, M.A. Garrido-Maneiro, C.J. Múnez, P. Poza, V. Utrilla, Surf. Coat. Technol. 204 (2009) 812.